

**This is the accepted manuscript version of the contribution published as:**

Cassarini, C., Rene, E.R., Bhattarai, S., **Vogt, C., Musat, N.**, Lens, P.N.L. (2019):  
Anaerobic methane oxidation coupled to sulfate reduction in a biotrickling filter: Reactor  
performance and microbial community analysis  
*Chemosphere* **236** , art. 124290

**The publisher's version is available at:**

<http://dx.doi.org/10.1016/j.chemosphere.2019.07.021>

# Accepted Manuscript

Anaerobic methane oxidation coupled to sulfate reduction in a biotrickling filter: reactor performance and microbial community analysis



Chiara Cassarini, Eldon R. Rene, Susma Bhattarai, Carsten Vogt, Niculina Musat, Piet N.L. Lens

PII: S0045-6535(19)31501-2  
DOI: 10.1016/j.chemosphere.2019.07.021  
Reference: CHEM 24290  
To appear in: *Chemosphere*  
Received Date: 11 March 2019  
Accepted Date: 02 July 2019

Please cite this article as: Chiara Cassarini, Eldon R. Rene, Susma Bhattarai, Carsten Vogt, Niculina Musat, Piet N.L. Lens, Anaerobic methane oxidation coupled to sulfate reduction in a biotrickling filter: reactor performance and microbial community analysis, *Chemosphere* (2019), doi: 10.1016/j.chemosphere.2019.07.021

This is a PDF file of an unedited manuscript that has been accepted for publication. As a service to our customers we are providing this early version of the manuscript. The manuscript will undergo copyediting, typesetting, and review of the resulting proof before it is published in its final form. Please note that during the production process errors may be discovered which could affect the content, and all legal disclaimers that apply to the journal pertain.

1 **Anaerobic methane oxidation coupled to sulfate reduction in a biotrickling**  
2 **filter: reactor performance and microbial community analysis**

3 Chiara Cassarini<sup>a,b\*</sup>, Eldon R. Rene<sup>a</sup>, Susma Bhattarai<sup>a</sup>, Carsten Vogt<sup>c</sup>, Niculina Musat<sup>c</sup> and Piet  
4 N. L. Lens<sup>a,b</sup>

5 <sup>a</sup> UNESCO-IHE, Institute for Water Education, P. O. Box 3015, 2601 DA, Delft, The  
6 Netherlands

7 <sup>b</sup> National University of Ireland Galway, University Road, Galway H91 TK33, Ireland

8 <sup>c</sup> Helmholtz-Centre for Environmental Research - UFZ, Department of Isotope Biogeochemistry,  
9 Permoser Strasse 15, 04318 Leipzig, Germany

10

11

12

13

14

15 \*Corresponding author

16 Chiara Cassarini

17 UNESCO-IHE, Institute for Water Education,

18 P. O. Box 3015, 2601 DA, Delft, the Netherlands

19 Phone: +353(0)830446104

20 E-mail: [chiara.cassarini@gmail.com](mailto:chiara.cassarini@gmail.com)

## 21 Abstract

22 The aim of this work was to evaluate the performance of a biotrickling filter (BTF) packed with  
23 polyurethane foam and pall rings for the enrichment of microorganisms mediating anaerobic  
24 oxidation of methane (AOM) coupled to sulfate reduction (SR) by activity tests and microbial  
25 community analysis. A BTF was inoculated with microorganisms from a known AOM active deep  
26 sea sediment collected at a depth of 528 m below the sea level (Alpha Mound, Gulf of Cadiz). The  
27 microbial community analysis was performed by catalysed reporter deposition - fluorescence in  
28 situ hybridization (CARD-FISH) and 16S rRNA sequence analysis. The AOM occurrence and  
29 rates in the BTF were assessed by performing batch activity assays using  $^{13}\text{C}$ -labelled methane  
30 ( $^{13}\text{CH}_4$ ). After an estimated start-up time of  $\sim 20$  days, AOM rates of  $\sim 0.3 \text{ mmol l}^{-1} \text{ day}^{-1}$  were  
31 observed in the BTF, values almost 20 times higher than previously reported in a polyurethane  
32 foam packed BTF. The microbial community consisted mainly of anaerobic methanotrophs  
33 (ANME-2, 22% of the total number of cells) and sulfate reducing bacteria (SRB, 47% of the total  
34 number of cells). This study showed that the BTF is a suitable reactor configuration for the  
35 enrichment of microbial communities involved in AOM coupled to SR at ambient pressure and  
36 temperature with a relatively short start-up time.

## 37 Highlights

- 38 • A biotrickling filter inoculated with deep-sea sediment performed anaerobic oxidation of  
39 methane coupled to sulfate reduction
- 40 • A short start-up (20 days) and high conversion rate ( $0.3 \text{ mmol l}^{-1} \text{ day}^{-1}$ ) were achieved
- 41 • Anaerobic methanotrophs and sulfate reducing bacteria were considerably enriched ( $\sim 70\%$   
42 of the total community) after 200 days of operation

43 **Keywords:** Biotrickling filter; anaerobic oxidation of methane; sulfate reduction; anaerobic  
44 methanotrophs; sulfate reducing bacteria; deep sea sediment.

## 45 1. Introduction

46 Anaerobic oxidation of methane (AOM) coupled to sulfate reduction (SR) is a biological process  
47 occurring in anoxic environments, especially in marine sediments (Reeburgh, 2007; Knittel and  
48 Boetius, 2009; Scheller et al., 2016). AOM contributes to the removal of methane, thereby  
49 controlling its emission to the atmosphere (Raghoebarsing et al., 2006; Reeburgh, 2007). Methane  
50 is a well-known greenhouse gas and its presence in the atmosphere at high concentrations has large  
51 implications for future climate change (Forster et al., 2007). Many terrestrial and aquatic surfaces  
52 are possible methane sources, thus, it is important to understand the processes and mechanisms  
53 involved in its consumption pattern in the environment (Kirschke et al., 2013).

54 AOM coupled to SR (AOM-SR) is a process mediated by anaerobic methanotrophs (ANME) and  
55 sulfate reducing bacteria (SRB). ANME-1, ANME-2 and ANME-3 are the three different types of  
56 ANME (Knittel and Boetius, 2009; Bhattarai et al., 2017a). All ANME are phylogenetically related  
57 to various groups of methanogenic archaea; it was recently shown how the ANME metabolism  
58 can be reversed to methanogenesis by only a few changes in carbon-metabolizing enzymes in  
59 ANME (McGlynn et al., 2017; Timmers et al., 2017). ANME are usually associated with different  
60 types of SRB, namely *Desulfosarcina/Desulfococcus* (DSS) or *Desulfobubaceae* (DBB)  
61 (Schreiber et al., 2010). AOM-SR is a well-known phenomenon occurring in anaerobic  
62 environments (Reeburgh, 2007; Knittel and Boetius, 2009; Scheller et al., 2016). However, the  
63 mode of cooperative interaction between ANME and SRB is still under debate and the difficulty  
64 in enriching the ANME under laboratory conditions hampers the investigation of the mechanism  
65 of this process. The main challenges for enrichment of ANME-SRB consortia are their slow

66 growth rates (doubling time of ~2 to 7 months), the low solubility of methane in water at standard  
67 atmospheric pressure and they are strictly anaerobic (Deusner et al., 2009; Meulepas et al., 2009a;  
68 Zhang et al., 2011; Wegener et al., 2016). Besides the biogeochemical implications of AOM, this  
69 microbial process can have biotechnological applications for the removal of sulfate from  
70 wastewater streams low in electron donors, using methane which is less costly and readily  
71 available. Moreover, the AOM process can be applied for nitrogen removal in wastewater with  
72 low levels of biodegradable organic matter. Sidestreams produced from anaerobic digestion for  
73 the production of biogas are rich in ammonium and lack organic matter (Rikmann et al., 2018;  
74 Zekker et al., 2018). Therefore, methane can be used as an electron donor and AOM can be applied  
75 to reduce nitrogen levels (Zhu et al., 2016) and for nutrient removal (e.g. nitrate and phosphorous)  
76 from wastewater (Mandel et al., 2019; Klein et al., 2017).

77 The enrichment of ANME can be enhanced by the use of different types of bioreactor  
78 configurations such as a high pressure reactor (Deusner et al., 2009; Zhang et al., 2011), membrane  
79 reactor (Meulepas et al., 2009a; Timmers et al., 2015a) or a biotrickling filter (Cassarini et al.,  
80 2017; Bhattarai et al., 2018b; Cassarini et al., 2018). However, the SR rates reported so far (~0.6  
81 mmol l<sup>-1</sup> day<sup>-1</sup>) with methane as the electron donor are more than 100 times lower than the rates  
82 achieved with other electron donors, such as hydrogen or ethanol (Suarez-Zuluaga et al., 2014;  
83 Bhattarai et al., 2017b). Moreover, a long start-up period is required for the bioreactor to perform  
84 AOM-SR, i.e. ~400 days for a membrane bioreactor inoculated with Eckenförde Bay sediment  
85 (Meulepas et al., 2009a).

86 In a recent study, Cassarini et al. (2018) operated a biotrickling filter (BTF) for 230 days with  
87 sediment collected from the Alpha Mound (Gulf of Cadiz, Spain) as inoculum. A BTF packed with  
88 polyurethane foam cubes was chosen to mimic the natural habitat of ANME and SRB to promote

89 their growth. These microorganisms have been found in carbonate-minerals, which is a porous  
90 matrix similar to the polyurethane foam (Marlow et al., 2014). The polyurethane foam provides  
91 good biomass retention, low shearing force, and high gas-liquid mass transfer (Cassarini et al.,  
92 2017). The high methane-liquid mass transfer will help retain the poorly soluble methane in the  
93 polyurethane pores (Aoki et al., 2014; Estrada et al., 2014).

94 Cassarini et al. (2018) showed that ANME and SRB obtained from deep sea conditions (528 m  
95 below sea level) can be enriched in a 0.4 l BTF at ambient pressure and temperature with a start-  
96 up time of 42 days. In that study, sulfate was reduced at a maximum rate of  $0.3 \text{ mmol l}^{-1} \text{ day}^{-1}$  and  
97 ANME-2 was enriched (7% of the total visualized archaea), but the AOM rate was  $\sim 10\%$  lower  
98 than the SR rate. However, the reactor start-up period was comparatively long for BTF reactors  
99 used for waste-gas treatment (Pérez et al., 2016), i.e.  $\sim 1\text{--}2$  weeks for a BTF used to treat methane  
100 emissions under oxic conditions (Avalos Ramirez et al., 2012; Estrada et al., 2014).

101 The aim of this study was, therefore, to further enrich this biomass from deep sea sediment in a  
102 6.6 l BTF packed with polyurethane foam cubes and pall rings to obtain higher AOM rates and  
103 thus, SR rates closer to the rates achieved with other electron donors, such as hydrogen or ethanol,  
104  $\sim 60 \text{ mmol l}^{-1} \text{ day}^{-1}$  (Suarez-Zuluaga et al., 2014; Bhattarai et al., 2017b). Batch activity assays using  
105  $^{13}\text{C}$ -labelled methane ( $^{13}\text{CH}_4$ ) were used to determine the AOM rate, whereas the growth of ANME  
106 and SRB cells was determined using catalyzed reporter deposition-fluorescence in situ  
107 hybridization (CARD-FISH) and analysis of 16S rRNA genes.

## 108 **2. Material and methods**

### 109 *2.1. Source of biomass and composition of the artificial seawater medium*

110 The enriched biomass after 230 days of incubation in a polyurethane sponge packed BTF  
111 (Cassarini et al., 2018) was used as inoculum for this study. The original sediment was obtained

112 from the Alpha Mound (35°17.48'N; 6°47.05'W, water depth ca. 525 m), Gulf of Cadiz (Spain),  
113 during the R/V Marion Dufresne Cruise MD 169 MiCROSYSTEMS to the Gulf of Cadiz in July  
114 2008. The characteristics of the sediment have been described in Cassarini et al. (2017). In brief,  
115 the Alpha Mound showed evidence for the presence of a shallow sulfate-methane transition zone  
116 driven by substantial methane fluxes and temperature varying between 10 and 15 °C (Wehrmann  
117 et al., 2011).

118 The artificial seawater mineral medium was composed of and prepared as described by Bhattarai  
119 et al. (2017a) with 10 mM of  $\text{SO}_4^{2-}$  added as  $\text{Na}_2\text{SO}_4$  in its anhydrous form (Fisher Scientific,  
120 Landsmeer, the Netherlands) as described previously (Cassarini et al. 2018). . Briefly, the vitamins  
121 and trace element mixtures were prepared according to Widdel and Bak (1992). 0.01 mM of  $\text{Na}_2\text{S}$   
122 was added as the reducing agent to the seawater mineral medium and 0.5 g l<sup>-1</sup> resazurin solution  
123 was added as the redox indicator. The pH of the seawater medium was adjusted to 7.0 with sterile  
124 1 M  $\text{Na}_2\text{CO}_3$  or 1 M  $\text{H}_2\text{SO}_4$  solution. The medium was maintained under anoxic conditions with  
125 the purging of nitrogen until it was recirculated to the BTF.

126 All the chemicals were purchased as lab grade from Fisher Scientific (Landsmeer, the  
127 Netherlands).

## 128 *2.2. BTF setup and operation*

129 The BTF (Figure 1) was a custom made cylindrical glass reactor (height: 62 cm, internal diameter:  
130 12 cm, total volume: 6.6 l), sealed air-tight to prevent leakages or air intrusion during its operation.  
131 The BTF was equipped with three sampling ports for the gas phase (inlet and outlet), the liquid  
132 phase and for the biomass (Figure 1). The filter bed volume of the BTF was 5.6 l which was packed  
133 with 76 g of polyurethane foam cubes of 1 cm<sup>3</sup> (0.98 void ratio and a density of 28 kg m<sup>-3</sup>) and  
134 230 g of polypropylene pall rings (0.87 void ratio and a density of 115 kg m<sup>-3</sup>). Two circular

135 acrylic sieve plates (pore size of 3.5 mm) were placed at the top of the BTF to facilitate  
136 homogeneous sprinkling of the medium and at the bottom to hold the polyurethane foam cubes  
137 (Figure 1).

138 The BTF was operated in sequential fed-batch mode for the trickling of artificial seawater medium,  
139 recirculating at a flow rate of  $10 \text{ ml min}^{-1}$  using a Masterflex S/L peristaltic pump (Metrohm  
140 Netherlands B.V, Schiedam, the Netherlands). The gas-phase methane (99.5% methane, Linde  
141 gas, Schiedam, the Netherlands) was supplied to the BTF by a gas sparger placed at the bottom of  
142 the BTF. The influent methane flow was measured and controlled by a Smart Thermal Mass Flow  
143 Controller (Brooks Instrument, Model SLA5850, Veenendaal, the Netherlands) at a constant flow  
144 rate of  $0.5 \text{ ml min}^{-1}$ , with a methane molar flow rate of  $29.6 \text{ mmol d}^{-1}$ , methane residence time  
145 with packing material of 8.7 days and methane loading rate of  $4.7 \text{ mmol l}^{-1} \text{ d}^{-1}$ . The outlet gas  
146 containing hydrogen sulfide, carbon dioxide and residual methane left the BTF via a gas cleaning  
147 bottle, which was filled with a  $0.5 \text{ M ZnCl}_2$  solution to selectively retain the hydrogen sulfide. The  
148 sulfide concentration in the bottle was measured once every 2 weeks. The pH of the BTF was  
149 monitored by a sulfide resistant pH electrode (Prosense, Oosterhout, The Netherlands).

150 550 ml of biomass ( $0.07 \pm 0.01 \text{ g}$  volatile suspended solids), pre-enriched by incubation for 230  
151 days in a 0.4 l acrylic BTF (Cassarini et al., 2018) was used to inoculate the BTF. The BTF was  
152 operated for 238 days in the dark, at atmospheric pressure and room temperature ( $\sim 20 \pm 2 \text{ }^\circ\text{C}$ )  
153 throughout the experimental period. The artificial seawater medium containing 10 mM sulfate was  
154 replaced periodically and the different operational phases of the BTF were defined by the medium  
155 replacement: days 0–61 (I), days 61–119 (II), days 119–160 (III), days 160–214 (IV) and days  
156 214–238 (V).

157 *2.3. Sampling*

158 Both gas (inlet and outlet) and liquid samples were collected twice a week from the sampling ports  
159 (Figure 1). pH, sulfate and sulfide concentrations were measured in samples collected from the  
160 liquid medium, while methane and carbon dioxide were analyzed from the gas samples collected  
161 at the inlet and outlet of the BTF. Biomass samples were collected in triplicate on day 112 and at  
162 the end of the BTF operation (day 238) for carrying out activity assays and analysis of microbial  
163 diversity by sequence analysis of 16S rRNA genes.

#### 164 *2.4. Activity assays*

165 The occurrence of AOM and the estimation of the methane oxidation rates were determined from  
166 the  $^{13}\text{C}$ -labeled carbon dioxide produced during batch tests with 5%  $^{13}\text{CH}_4$  following the procedure  
167 described by Cassarini et al. (2018). The polyurethane foam cubes containing the enriched  
168 inoculum were collected from the BTF at the end of its operation. The tests were performed in  
169 triplicate to evaluate the standard deviation. Control batch experiments were prepared under  
170 nitrogen atmosphere (without methane), in the absence of the electron acceptor and without the  
171 biomass (fresh polyurethane foam cubes were added).

172 The bottles were placed on an orbital shaker (Cole-Parmer, Germany) at 100 rpm in the dark at the  
173 operation temperature of the BTF ( $20 \pm 2$  °C) for 42 days. Sampling was performed once a week  
174 for both gas and liquid phase analysis as well as CARD-FISH analysis (only 4 time points: 0, 21,  
175 28 and 42 days).

#### 176 *2.5. Chemical analysis*

177 Samples for analysis of pH, sulfate, thiosulfate and dissolved sulfide concentrations were analyzed  
178 at least in duplicate. The pH, sulfate, thiosulfate, methane and carbon dioxide concentrations were  
179 analyzed according to the procedure described in Cassarini et al. (2017). The total dissolved sulfide

180 concentrations ( $\text{H}_2\text{S}$ ,  $\text{HS}^-$  and  $\text{S}^{2-}$ ) in the BTF were analyzed spectrophotometrically using the  
181 methylene blue method (Acree et al., 1971). The volumetric AOM, SR and the total dissolved  
182 sulfide production rates were determined for each phase of the BTF. The data points of the different  
183 compound (methane, sulfate and total dissolved sulfide) concentrations were fitted to a zero-order  
184 rate equation using the least square method ( $R^2 > 0.97$ ). The mass balance of carbon and sulfur  
185 was calculated on the basis of the concentration of carbon/sulfur compounds entering and leaving  
186 the BTF during every operational phase. The mass balance was calculated in terms of mM of  
187 carbon/sulfur recovered and also in fractions of different sulfur/carbon compounds formed during  
188 the different phases.

189 The stable carbon isotope composition of methane and carbon dioxide were determined using a  
190 gas chromatography - isotope ratio mass spectrometer (GC-IRMS, Agilent 7890A) as described  
191 by Herrmann et al. (2010). Ratios of stable carbon isotopes ( $^{13}\text{C}/^{12}\text{C}$ ) were estimated as described  
192 by Dorer et al. (2016). Measurements of the stable isotope composition of methane and carbon  
193 dioxide were performed in triplicate and the standard deviation was observed to be less than 0.5  
194  $\delta$ -units. For quality assurance, standard gas mixtures of methane and carbon dioxide were  
195 measured periodically during the entire isotopic analysis. The AOM rate was estimated on the  
196 basis of the dissolved inorganic carbon (DIC) produced from  $^{13}\text{CH}_4$  during the activity assays as  
197 described by Cassarini et al. (2018).

198 The volatile suspended solids (VSS) were estimated before inoculation on the basis of the  
199 difference between the dry and ash weights of the sediment according to the procedure outlined in  
200 Standard Methods (APHA 2012).

201 *2.6. DNA extraction*

202 DNA was extracted using a FastDNA<sup>®</sup> SPIN Kit for soil (MP Biomedicals, Solon, OH, USA)  
203 following the manufacturer's protocol. Approximately 0.5 g of the sediment was used for DNA  
204 extraction from the initial inoculum and ~0.5 ml of liquid obtained by washing the polyurethane  
205 foam packing with nuclease free water was used for extracting the DNA from the BTF biomass.  
206 The extracted DNA was quantified and its quality was checked according to the procedure outlined  
207 by Bhattarai et al. (2017a).

### 208 *2.7. Polymerase chain reaction (PCR) amplification for 16S rRNA genes and Illumina Miseq data* 209 *processing*

210 The DNA was amplified using the bar coded archaea specific primer pair Arc516F (forward) and  
211 Arc855R (reverse). The primer pairs used for bacteria were forward bac520F 5' -3' AYT GGG  
212 YDT AAA GNG and reverse Bac802R 5' -3' TAC NNG GGT ATC TAA TCC (Song et al., 2013).  
213 The PCR reaction mixture was prepared as described by Bhattarai et al. (2017a), whereas the PCR  
214 amplification for bacteria and archaea was performed as described by Cassarini et al. (2019).  
215 After checking the correct band size, 150 µl of PCR amplicons were loaded in 1% agarose gel and  
216 electrophoresis was performed for 120 min at 120 V. The gel bands were excited under UV light  
217 and the PCR amplicons were cleaned using the E.Z.N.A.<sup>®</sup> Gel Extraction Kit by following the  
218 manufacturer's protocol (Omega Biotek, USA). The purified DNA amplicons were sequenced by  
219 an Illumina HiSeq 2000 (Illumina, San Diego, USA) and analyzed according to the detailed  
220 analytical procedure described in Bhattarai et al. (2017a).

221 A total of 40,000 ( $\pm$  20,000) sequences were assigned to archaea and bacteria by examining the  
222 tags assigned to the amplicons for at least duplicate (one sample did not contain enough number  
223 of sequences, i.e. < 10,000, for the analysis) DNA samples extracted from the BTF biomass at the

224 start and the end of the BTF operation. More details on the analytical procedure have been  
225 described by Bhattarai et al. (2017a). After eliminating the chimeras, the sequences for archaea  
226 and bacteria were analyzed and classified in MOTHUR (Schloss and Westcott, 2011). Briefly  
227 stating, the faulty sequences with mismatch tags or primers and with a size <200 bp were removed  
228 by using the shhh.flows command. Therefore, the putative chimeric sequences were identified and  
229 removed by the chimera.uchime command using the most abundant reads in the respective  
230 sequence data sets as references. Assembled reads that passed the chimera checking were clustered  
231 into the new operational taxonomic units (OTUs) at a cut off of 97% sequence similarity. Finally,  
232 the sequence reads were classified according to the SILVA taxonomy database version 121  
233 (Pruesse et al., 2007) using the classify.seqs command and the relative sequence abundance of  
234 each phylotype was assessed. These sequence data were submitted to the NCBI GenBank database  
235 under the BioProject accession number PRJNA415004 (direct link:  
236 <http://www.ncbi.nlm.nih.gov/bioproject/415004>).

### 237 *2.8. Cells visualization and counting by CARD-FISH*

238 Analysis of single cells in biomass samples collected from the BTF and from the activity assays  
239 were performed by CARD-FISH as described by Cassarini et al. (2017) and Cassarini et al. (2018).  
240 For dual-CARD-FISH, peroxidases of initial hybridizations were inactivated according to the  
241 procedure described in Holler et al. (2011). Tyramide amplification was performed using the  
242 fluorochromes Oregon Green 488-X and Alexa Fluor 594, which were prepared according to the  
243 procedure outlined in Pernthaler et al. (2004).

244 The microorganisms were visualized using archaeal and bacterial HRP-labeled oligonucleotide  
245 probes ARCH915 (Stahl and Amann, 1991) and EUB338-I-III (Daims et al., 1999), respectively.  
246 The probes DSS658 (Manz et al., 1998) and ANME-2 538 (Schreiber et al., 2010) were used for

247 the detection of DSS and ANME-2 cells, respectively. Oligonucleotide probes were purchased  
248 from Biomers (Ulm, Germany).

249 Total cells were counterstained with 4',6'-diamidino-2-phenylindole (DAPI) and visualized using  
250 an epifluorescence microscope (Carl Zeiss, Germany). Cell counting was performed as described  
251 by Cassarini et al. (2019), 700-1,000 DAPI-stained cells and their corresponding probe fluorescent  
252 signals for each probe per incubation (triplicate) were counted as described previously in the  
253 literature (Musat et al., 2008; Kleindienst et al., 2012). Cell counts are indicated as the average  $\pm$   
254 standard deviation of triplicate samples. The statistical data analysis was performed using SPSS  
255 25.0 (IBM, USA). Significant differences were determined by one-way ANOVA and post-hoc  
256 analysis for multiple group comparison (Tukey HSD). Differences were considered to be  
257 significant at  $p \leq 0.05$ . The homogeneity of the variance of the parameters was evaluated using a  
258 Levene test.

### 259 **3. Results and discussion**

#### 260 *3.1. Performance of the BTF*

##### 261 *3.1.1. Start-up time of the BTF*

262 The long start-up time of the AOM-SR process is one of the major drawbacks for its application  
263 in the treatment of wastewaters and groundwater (Meulepas et al., 2009a). In previous studies,  
264 start-up periods of  $\sim 400$  days (Meulepas et al., 2009a) and  $\sim 365$  days (Aoki et al., 2014) have been  
265 reported in a membrane bioreactor and hanging sponge reactor, respectively. The estimated AOM-  
266 SR start-up time in this study was only 20 days (Figure 2), much shorter than what was previously  
267 reported and comparable to the start-up period ( $\sim 1$ -2 weeks) of a BTF used to treat methane  
268 emissions under aerobic conditions (Avalos Ramirez et al., 2012; Estrada et al., 2014, Pérez et al.,  
269 2016). Recently, Cassarini et al. (2018) showed that the polyurethane foam packed BTF (without

270 pall rings) is a suitable bioreactor for the enrichment of slow growing microorganisms reducing  
271 the start-up time (120 days) to more than half of what was previously reported (~400 days). This  
272 study showed that the start-up period of AOM-SR BTF can be further reduced by using an enriched  
273 AOM-SR biomass and a mix of polyurethane foam and pall rings as the packing material.

### 274 3.1.2. Sulfate reduction rates

275 The maximum SR rates obtained ( $0.3 \text{ mmol l}^{-1} \text{ day}^{-1}$ ) were similar to the rates previously achieved  
276 in BTFs packed with only polyurethane foam (Cassarini et al., 2018; Bhattarai et al., 2018b). In  
277 phase I, 3 mM of sulfate was consumed after 20 days of reactor operation (start-up period), while  
278 sulfide was only scarcely produced (0.9 mM) towards the end of phase I (Figure 2B). In the first  
279 two phases (phases I and II), the SR and sulfide production rates were low (Figure 2B and Table  
280 1) and not all the sulfate reduced was recovered as sulfide, i.e. 33% (phase I) and 61% (phase II).  
281 As previously described (Cassarini et al., 2018), part of the dissolved sulfide could have been  
282 precipitated as metal sulfide or could have been oxidized to elemental sulfur due to the presence  
283 of iron oxides in the Alpha Mound sediment (Wehrmann et al., 2011). Other sulfur compounds,  
284 such as polysulfides, could have also been formed, which were not analyzed in this study.

285 The highest SR rates were obtained in the last three phases of the BTF operation (Figure 2B and  
286 Table 1) and around 80% of the sulfate was reduced during each phase. The SR and sulfide  
287 production rates in the last three phases are not significantly different from each other (one-way  
288 ANOVA:  $p > 0.050$ ). In phase III, the SR and sulfide production rates were  $0.29 \text{ mmol l}^{-1} \text{ day}^{-1}$   
289 and  $0.17 \text{ mmol l}^{-1} \text{ day}^{-1}$ , respectively. On day 133, almost all sulfate reduced was recovered as  
290 total dissolved sulfide (96%). However, the total dissolved sulfide concentration decreased  
291 abruptly from 4.7 to 2.1 mM on day 147 until the end of phase III, while the concentration of  
292 sulfate kept decreasing. This is probably due to polysulfides formation during this period: the

293 abrupt increase in the dissolved sulfide concentration on day 140 and the alkaline pH (8.3) favored  
294 polysulfide formation (Finster et al., 1998). This assumption is supported by the change of color of  
295 the mineral medium (yellow) observed from day 150 until the replacement of fresh medium (160  
296 days).

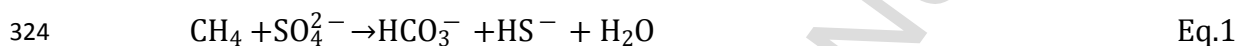
297 In phases IV and V, the total dissolved sulfide concentration increased to values as high as 6.6  
298 mM. The SR rate ranged between 0.26 and 0.29 mmol l<sup>-1</sup> day<sup>-1</sup> during the last two phases of the  
299 BTF operation, similarly to phase III. The sulfide production rate was 0.17 mmol l<sup>-1</sup> day<sup>-1</sup> in phase  
300 IV, the same as in phase III. Differently in phase V, the sulfide production rate was lower: 0.15  
301 mmol l<sup>-1</sup> day<sup>-1</sup>. The pH of the BTF increased from 7.5 to 8.3 in all the five phases of the reactor  
302 operation (Figure 2A). The pH was brought down to 7.5 at each starting phase due to the mineral  
303 medium replacement, but increased to 8.3 due to the sulfide production. pH changes can cause  
304 disturbance on the microbial community mediating the target process (Tenno et al., 2018). The  
305 optimum pH for ANME and SRB is between 7 and 8 (Meulepas et al., 2009b). A pH higher than  
306 9 or lower than 6.5 can substantially decrease the SR rate. However, in the last three phases of the  
307 BTF operation the pH ranged from 7.5 to 8.4 (in phase V), but the SR rate did not significantly  
308 change.

309 Nonetheless, the performance of the BTF can be further improved and customized to treat sulfur  
310 compounds other than sulfate, or other unwanted compounds such as selenium for future  
311 biotechnology applications.

### 312 *3.1.3. Methane oxidation rates*

313 As reported in Table 1 and shown in Figure 2C, differently than the SR rate, the methane  
314 consumption rate was higher than previously reported in BTF systems performing AOM, in which

315 the AOM rates were ten times lower than the SR rates (Bhattarai et al., 2018b; Cassarini et al.,  
316 2018). The methane consumption rate was the highest in the last three phases (III, IV and V) of  
317 the BTF operation, similar to the SR rates, but in phase IV and V the AOM rate was significantly  
318 higher than the SR in the corresponding phases (determined by one-way ANOVA:  $p = 0.011$  and  
319  $p = 0.001$ , respectively), showing that the stoichiometry of the reaction for AOM-SR (Eq. 1) was  
320 not followed. During the BTF operation, the reported methane consumption rate corresponds to  
321 the net methane consumption but it does not correspond to the net sulfate dependent-AOM.  
322 Previous studies showed that if net methane production (methanogenesis) occurs, trace amounts  
323 of methane will be concomitantly oxidized (Timmers et al., 2015b), leading to higher AOM rates.



325 Similar to the SR rates, the AOM rates did not significantly change during the last three phases of  
326 the BTF operation (one-way ANOVA:  $p > 0.050$ ), showing that, from day 54 until the end of the  
327 operation the BTF reactor, the AOM-mediating microorganisms performed AOM-SR at similar  
328 volumetric rates at ambient temperature and pressure in the BTF.

#### 329 *3.1.4. Carbon dioxide production*

330 The amount of carbon dioxide produced was the highest in phase III and IV (Figure 2C), when  
331 sulfide production was also the highest (6.6 mM). However, this amount corresponds to the net  
332 carbon dioxide concentration and does not account for the carbon dioxide production from sources  
333 other than methane or for its utilization by microorganisms. ANME, especially ANME-1, were  
334 found to utilize carbon dioxide as a carbon source (Treude et al., 2007; Holler et al., 2011).  
335 However, hardly any ANME-1 sequences were retrieved by 16S rRNA gene sequence analysis, as  
336 further discussed in the following section.

337 The carbon mass balance showed that the carbon recovery for each phase of the reactor operation  
338 was between 76 and 99% (Table 1), the majority of the methane entering the BTF escaped as  
339 methane-outgas from the BTF due to its low solubility in the artificial seawater medium (1.3 mM  
340 in seawater at 20°C). Only a small amount of carbon (around 3%) accounts for the dissolved  
341 methane, which was mostly converted to carbon dioxide by AOM-SR. In order to account for the  
342 potential formation of methane and trace methane oxidation due to methanogenesis and carbon  
343 dioxide production from sources other than methane, batch activity assays with the enriched  
344 biomass after 238 days of BTF operation were performed, and the results are shown and discussed  
345 in section 3.3.

### 346 *3.2. Archaeal and bacteria diversity in the BTF*

347 Figure 3 shows the microbial community profiles obtained at the start and at the end of BTF  
348 operation (238 days). The highest percentages of archaeal 16S rRNA reads are shown in Figure  
349 3A. Among the ANME clades, ANME-2a/b comprised 37% of the archaeal reads at the start and  
350 60% at the end of the BTF operation. Other ANME clades, such as ANME-1, were also retrieved  
351 but the relative abundance was very low, from 0.08 to 0.01%, while the relative abundance of  
352 ANME-3 increased from 0.09 to 0.5%. More than 60% of the retrieved archaeal sequences belong  
353 to the ANME group, which reflects the high AOM rate obtained in the BTF. ANME-2 was the  
354 most abundant ANME type as in the previously reported studies using Alpha Mound sediment in  
355 a BTF (Cassarini et al., 2017; Cassarini et al., 2018), but also in other AOM studies performed in  
356 continuous bioreactor enrichments either at ambient (Meulepas et al., 2009a) or elevated (Zhang  
357 et al., 2011) pressure. However, ANME-1 cells were enriched in a similar BTF performing AOM  
358 by the Gingsburg Mud Volcano sediment (Bhattarai et al., 2018b). Different factors can influence  
359 the growth of ANME types, such as the availability of the substrates (e.g. methane and sulfate),

360 their mode of transport, the temperature and pressure, which can influence their availability.  
361 However, the microbial and chemical composition of the inoculum also plays a major role and can  
362 reflect the growth of the different microorganisms.

363 The bacterial community was more diverse at the start, where the relative abundance of other  
364 different bacteria (“other bacteria” in Figure 3B) was 19%, much higher than at the end (238 days  
365 of BTF operation), where the abundance of “other bacteria” was 0.1 % (Figure 3B). Bacteria that  
366 could not compete in the AOM-SR environment in the BTF almost disappeared, such as  
367 *Marinobacter* (Figure 3B). A high sulfate reducing activity was recorded in the BTF,  
368 corresponding to a high percentage of bacterial 16S rRNA reads belonging to the order of  
369 *Desulfobacterales* (Figure 3B), especially the relative percentage of *Desulfosarcina* increased  
370 (from 36% to 58%). Other bacterial sequences from the *Deltaproteobacteria* class, such as  
371 *Desulfarculus* and *Desulfuromonas*, were retrieved as well (Figure 3B). The relative percentage of  
372 the *Desulfarculus* increased from less than 0.01 to 11% and the relative percentage of  
373 *Desulfuromonas* increased from less than 1 to 10%. *Desulfuromonas* are elemental sulfur and  
374 polysulfides reducers (Schauer et al., 2011), which gives a further indication of possible formation  
375 of polysulfides in the BTF and their further reduction.

### 376 3.3. AOM activity

377 During the activity assays with  $^{13}\text{CH}_4$  using the biomass from the BTF, 95% of the reduced sulfate  
378 was recovered as total dissolved sulfide (Figure 4A). In the control incubation without biomass  
379 (Figure 4A, dashed lines), sulfide was not produced, while in the batch incubations without  
380 methane (Figure 4A, dotted lines), sulfide was produced only until day 20 (1.7 mM).

381 In the first 20 days of activity assays, the SR and sulfide production rate for the samples and control  
382 without methane were not significantly different (Table 1). Enriched biomass entrapped in the  
383 polyurethane foam cubes from the BTF operated for 238 days with a constant supply of methane  
384 was used for all the batches and control without methane during the activity assays. Most likely  
385 the enriched microorganisms mediating AOM-SR continued to reduce sulfate from endogenous  
386 carbon sources, even without the further addition of methane for 20 days.

387 The total DIC produced from methane increased only in the incubations with the biomass from  
388 the BTF and in the presence of methane in the headspace to 5.36 mM (Figure 4B). The calculated  
389 AOM was  $0.16 \text{ mmol l}^{-1} \text{ day}^{-1}$ , which was higher than the SR ( $0.10 \text{ mmol l}^{-1} \text{ day}^{-1}$ ) and sulfide  
390 ( $0.09 \text{ mmol l}^{-1} \text{ day}^{-1}$ ) production rates during the activity assays (Table 1). No methane was  
391 produced in the control without methane, confirming that no methanogenic activity occurred in  
392 the batches. Therefore,  $0.16 \text{ mmol l}^{-1} \text{ day}^{-1}$  is the net AOM occurring in the activity assays,  
393 excluding carbon dioxide from sources other than methane and trace methane oxidation. In 42  
394 days, 5 mM of sulfate were consumed and 5 mM of DIC were produced following the reaction  
395 stoichiometry (Eq. 1). The AOM rate found in this study was almost 20 times higher than that  
396 previously found after enrichment in a polyurethane foam packed BTF for 230 days (Cassarini et  
397 al., 2018), due to the further enrichment of ANME from the Alpha Mound sediment (Table 2).

#### 398 *3.4. Cell numbers of ANME-2 and DSS*

399 ANME-2 and DSS were the most abundant microorganisms mediating AOM-SR in a previously  
400 reported BTF inoculated with Alpha Mound sediment (Cassarini et al., 2017; Cassarini et al.,  
401 2018). In this study, higher numbers of ANME-2 and DSS (22% and 55%, respectively) compared  
402 to previous studies (7% of ANME-2 and 46% of DSS) were found after 238 days in the BTF  
403 packed with polyurethane foam and pall rings and after 42 days of activity assays (Figure 5).

404 The cocci-shaped ANME-2 cells were mostly visualized in the form of aggregates (Figure 5A and  
405 5C), but also ANME-2 clusters without bacterial partner were visualized (Figure 5B). The DSS  
406 cells were present in different shapes, either as cocci usually surrounded with ANME-2 (Figure  
407 5A, 5C and 4D), e) or vibrio shaped, usually visualized without archaeal partner (Figure 5B). The  
408 cooperative interaction between ANME-2 and DSS is suggested in this study by their more  
409 common visualization in aggregates (Figure 5A, 5C and 5D). However, ANME-2 have been  
410 visualized without bacterial partner before, as more rarely found in this study (Figure 5B),  
411 suggesting that this ANME type is supporting a metabolism independent of an obligatory bacterial  
412 association (Ruff et al., 2016). The cooperative interaction between the ANME-2 and DSS is still  
413 under debate: Milucka et al. (2012) stated that a syntrophic partner might not be required for  
414 ANME-2 and that they can be decoupled by using external electron acceptors (Scheller et al.,  
415 2016), whereas recent studies have shown direct electron transfer between the two (ANME-2 and  
416 DSS) partners (McGlynn et al., 2015; Wegener et al., 2015).

417 The number of cells stained with specific CARD-FISH probes were counted along the incubation  
418 time during the activity assays (Figure 5E). The number of cells stained with the bacterial CARD-  
419 FISH probe (EUB 338-I-II-III) was always higher than the number of stained archaeal cells (Figure  
420 5E). A significant decrease in the bacterial population was registered from the start of the activity  
421 assays till day 21 (one-way ANOVA:  $p = 0.047$ ) and till day 28 (one-way ANOVA:  $p = 0.003$ ).  
422 The samples were successfully hybridized with the DSS probe and with the ANME-2 probe,  
423 separately. The cells hybridized with the DSS probe were always significantly more abundant than  
424 the ANME-2 cells. However, there was no significant difference in the DSS population from the  
425 start till the end of the activity assays (one-way ANOVA:  $p > 0.050$ ). The DSS were ~42 % of the  
426 total number of the stained cells during the activity assays (Figure 5E).

427 The archaeal population did not change significantly during the activity assays (one-way ANOVA:  
428  $p > 0.050$ ) and the number of ANME-2 visualized and counted is close to the total number of  
429 archaea. However, ANME-2 significantly increased (22% of the total number of stained cells)  
430 from the start of the activity assays till day 28 (one-way ANOVA:  $p = 0.000$ ) and from the  
431 beginning till day 42 (one-way ANOVA:  $p = 0.020$ ).

432 The visualization and quantification of ANME-2 and DSS, supposedly mediating AOM-SR,  
433 confirmed that further enrichment of the anaerobic methanotrophs, specifically ANME-2, occurred  
434 during the BTF operation with polyurethane foam and pall rings as packing material following the  
435 increase in the AOM rate compared to the previously reported BTF (Cassarini et al., 2018).

#### 436 **4. Conclusions and implications**

437 This study indicated that a BTF packed with polyurethane foam and pall rings inoculated with  
438 enriched biomass showed a rapid start-up (~20 days) and a better performance in terms of AOM-  
439 rates ( $0.4 \text{ mmol l}^{-1} \text{ day}^{-1}$ ) and ANME-2 (22%) and DSS (50%) enrichment. This is the highest  
440 AOM rate reported so far in a BTF system inoculated with deep sea sediment. However, the SR  
441 rate should still be 100 times higher than what was found in this study to be competitive with the  
442 SR rates achieved for desulfurization of wastewater with other electron donors, such as hydrogen  
443 or ethanol.

444 The BTF technology is widely used for the treatment of industrial waste gases containing volatile  
445 organic and inorganic pollutants, however, its main disadvantage is clogging due to the  
446 accumulation of excess biomass. The BTF used in this study did not pose any operational problem  
447 with respect to clogging or channeling, and the biomass was actively maintained during its long  
448 term operation (230 days). The BTF design for AOM-SR can be nevertheless further optimized.

449 The majority of the methane entering the BTF escaped as methane outgas from the BTF due to its  
450 low solubility in the artificial seawater medium. A gas-recycling strategy could be used to enhance  
451 the CH<sub>4</sub> gas to liquid-phase mass transfer even at low concentrations of CH<sub>4</sub>. In the BTF for AOM-  
452 SR, recycling the non-oxidized CH<sub>4</sub> to achieve its complete removal might be a good approach.  
453 However, unwanted or toxic compounds, such as hydrogen sulfide, need to be stripped out prior  
454 recirculation.

455 For future applications, naturally occurring materials (e.g. sandstone, lava rocks) or inert materials  
456 such as plastic rings or resins can be tested in a BTF for AOM-SR. Based on the knowledge gained  
457 from this work, ANME and SRB can be enriched in a BTF. The enriched community can be further  
458 used to understand its mechanisms and the BTF design can be further improved and controlled for  
459 future biotechnological applications of AOM-SR.

460

#### 461 **Acknowledgments**

462 We acknowledge Dr. Yu Zhang and the State Key Laboratory of Microbial Metabolism from  
463 Shanghai Jiao Tong University (Shanghai, China) for providing the sediment from Alpha Mound  
464 (Gulf of Cadiz) and the required analytical facilities for carrying out the microbial phylogenetic  
465 analysis. The authors acknowledge the support received from the Centre for Chemical Microscopy  
466 (ProVIS) at the Helmholtz-Centre for Environmental Research, which is supported by the  
467 European Regional Development Funds (ERDF and Europe funds Saxony) and the Helmholtz  
468 Association. This research was funded by the Erasmus Mundus Joint Doctorate Programme  
469 ETeCoS<sup>3</sup> (Environmental Technologies for Contaminated Solids, Soils and Sediments) under the  
470 grant agreement FPA no. 2010-0009.

#### 471 **References**

- 472 Acree, T.E., Sonoff, E.P., Splittstoesser, D.F., 1971. Determination of hydrogen sulfide in  
473 fermentation broths containing SO<sub>2</sub>. *Appl. Microbiol.* 22, 110-112.
- 474 Aoki, M., Ehara, M., Saito, Y., Yoshioka, H., Miyazaki, M., Saito, Y., Miyashita, A., Kawakami,  
475 S., Yamaguchi, T., Ohashi, A., Nunoura, T., Takai, K., Imachi, H., 2014. A long-term cultivation  
476 of an anaerobic methane-oxidizing microbial community from deep-sea methane-seep sediment  
477 using a continuous-flow bioreactor. *Plos One* 9, e105356.
- 478 APHA., 2012. Standard methods for the examination of water and wastewater, in: American Public  
479 Health Association, 19<sup>th</sup> ed. Washington DC, USA. pp.1325.
- 480 Avalos Ramirez, A., Jones, J.P., Heitz, M., 2012. Methane treatment in biotrickling filters packed  
481 with inert materials in presence of a non-ionic surfactant. *J. Chem. Technol. Biotechnol.* 87, 848-  
482 853.
- 483 Bhattarai, S., Cassarini, C., Gonzalez-Gil, G., Egger, M., Slomp, C.P., Zhang, Y., Esposito, G.,  
484 Lens, P.N.L., 2017a. Anaerobic methane-oxidizing microbial community in a coastal marine  
485 sediment: anaerobic methanotrophy dominated by ANME-3. *Microb. Ecol.* 74, 608-622.
- 486 Bhattarai, S., Cassarini, C., Naangmenyele, Z., Rene, E.R., Gonzalez-Gil, G., Esposito, G., Lens,  
487 P.N.L., 2017b. Microbial sulfate reducing activities in anoxic sediment from Marine Lake  
488 Grevelingen. *Limnology*. <https://doi.org/10.1007/s10201-017-0516-0>.
- 489 Bhattarai, S., Cassarini, C., Rene, E.R., Kümmel, S., Esposito, G., and Lens, P.N.L., 2018a.  
490 Enrichment of ANME-2 methanotrophy from cold seep sediment in an external ultrafiltration  
491 tration membrane bioreactor. *Eng. Life Sci.* 18, 368.
- 492 Bhattarai, S., Cassarini, C., Rene, E.R., Zhang, Y., Esposito, G., and Lens, P.N., 2018b.  
493 Enrichment of sulfate reducing anaerobic methane oxidizing community dominated by ANME-1  
494 from Ginsburg Mud Volcano (Gulf of Cadiz) sediment in a biotrickling filter. *Bioresour. Technol.*  
495 259, 433-441.
- 496 Cassarini, C., Bhattarai, S., Rene, E.R., Vogt, C., Musat, N., Esposito, G., Lens, P.N.L., 2018.  
497 Enrichment of anaerobic methanotrophs in biotrickling filters using different sulfur compounds as  
498 electron acceptor. *Environ. Eng. Sci.* <https://doi.org/10.1089/ees.2018.0283>.
- 499 Cassarini, C., Rene, E.R., Bhattarai, S., Esposito, G., Lens, P.N.L., 2017. Anaerobic oxidation of  
500 methane coupled to thiosulfate reduction in a biotrickling filter. *Bioresour. Technol.* 240, 214-222.
- 501 Cassarini, C., Zhang, Y., Lens, P.N. L., 2019. Pressure selects dominant anaerobic methanotrophic  
502 phylotype and sulfate reducing bacteria in coastal marine lake Grevelingen sediment. *Front.*  
503 *Environ. Sci.* 6, 162.
- 504 Daims, H., Brühl, A., Amann, R., Schleifer, K.-H., Wagner, M., 1999. The domain-specific probe  
505 EUB338 is insufficient for the detection of all Bacteria: development and evaluation of a more  
506 comprehensive probe set. *Syst. Appl. Microbiol.* 22, 434-444.

- 507 Deusner, C., Meyer, V., Ferdelman, T., 2009. High-pressure systems for gas-phase free continuous  
508 incubation of enriched marine microbial communities performing anaerobic oxidation of methane.  
509 Biotechnol. Bioeng. 105, 524-533.
- 510 Dorer, C., Vogt, C., Neu, T.R., Stryhanyuk, H., Richnow, H.H., 2016. Characterization of toluene  
511 and ethylbenzene biodegradation under nitrate-, iron (III)-and manganese (IV)-reducing  
512 conditions by compound-specific isotope analysis. Environ. Pollut. 211, 271-281.
- 513 Estrada, J.M., Dudek, A., Muñoz, R., Quijano, G., 2014. Fundamental study on gas-liquid mass  
514 transfer in a biotrickling filter packed with polyurethane foam. J. Chem. Technol. Biotechnol. 89,  
515 1419-1424.
- 516 Finster, K., Liesack, W., Thamdrup, B., 1998. Elemental sulfur and thiosulfate disproportionation  
517 by *Desulfocapsa sulfoexigens* sp. nov., a new anaerobic bacterium isolated from marine surface  
518 sediment. Appl. Environ. Microbiol. 64, 119-125.
- 519 Forster, A., Schouten, S., Baas, M., Sinninghe Damsté, J.S., 2007. Mid-Cretaceous (Albanian-  
520 Santonian) sea surface temperature record of the tropical Atlantic Ocean. Geology 35, 919.
- 521 Herrmann, S., Kleinsteuber, S., Chatzinotas, A., Kuppardt, S., Lueders, T., Richnow, H.-H., Vogt,  
522 C., 2010. Functional characterization of an anaerobic benzene-degrading enrichment culture by  
523 DNA stable isotope probing. Environ. Microbiol. 12, 401-411.
- 524 Holler, T., Widdel, F., Knittel, K., Amann, R., Kellermann, M.Y., Hinrichs, K.-U., Teske, A.,  
525 Boetius, A., Wegener, G., 2011. Thermophilic anaerobic oxidation of methane by marine  
526 microbial consortia. ISME J. 5, 1946-1956.
- 527 Kirschke, S., Bousquet, P., Ciais, P., Saunois, M., Canadell, J.G., Dlugokencky, E.J.,  
528 Bergamaschi, P., Bergmann, D., Blake, D.R., Bruhwiler, L., Cameron-Smith, P., Castaldi, S.,  
529 Chevallier, F., Feng, L., Fraser, A., Heimann, M., Hodson, E.L., Houweling, S., Josse, B., Fraser,  
530 P.J., Krummel, P.B., Lamarque, J.-F., Langenfelds, R.L., Le Quéré, C., Naik, V., O'Doherty, S.,  
531 Palmer, P.I., Pison, I., Plummer, D., Poulter, B., Prinn, R.G., Rigby, M., Ringeval, B., Santini, M.,  
532 Schmidt, M., Shindell, D.T., Simpson, I.J., Spahni, R., Steele, L.P., Strode, S.A., Sudo, K., Szopa,  
533 S., van der Werf, G.R., Voulgarakis, A., van Weele, M., Weiss, R.F., Williams, J.E., Zeng, G.,  
534 2013. Three decades of global methane sources and sinks. Nat. Geosci. 6, 813-823.
- 535 Klein, K., Kivi, A., Dulova, N., Zekker, I., Mölder, E., Tenno, T., Trapido, M., Tenno, T., 2017.  
536 A pilot study of three-stage biological–chemical treatment of landfill leachate applying continuous  
537 ferric sludge reuse in Fenton-like process. Clean Techn. Environ. Policy 19, 541-551.
- 538 Kleindienst, S., Ramette, A., Amann, R., Knittel, K., 2012. Distribution and in situ abundance of  
539 sulfate-reducing bacteria in diverse marine hydrocarbon seep sediments. Environ. Microbiol. 14,  
540 2689-710.
- 541 Knittel, K., Boetius, A., 2009. Anaerobic oxidation of methane: progress with an unknown process.  
542 Annual. Rev. Microbiol. 63, 311-334.

- 543 Mandel, A., Zekker, I., Jaagura, M., Tenno, T., 2019. Enhancement of anoxic phosphorus uptake  
544 of denitrifying phosphorus removal process by biomass adaption. *Int. J. Environ. Sci. Technol.*  
545 <https://doi.org/10.1007/s13762-018-02194-2>.
- 546 Manz, W., Eisenbrecher, M., Neu, T.R., Szewzyk, U., 1998. Abundance and spatial organization  
547 of gram-negative sulfate-reducing bacteria in activated sludge investigated by in situ probing with  
548 specific 16S rRNA targeted oligonucleotides. *FEMS Microbiol. Ecol.* 25, 43-61.
- 549 Marlow, J.J., Steele, J.A., Case, D.H., Connon, S.A., Levin, L.A., Orphan, V.J., 2014. Microbial  
550 abundance and diversity patterns associated with sediments and carbonates from the methane seep  
551 environments of Hydrate Ridge, OR. *Front. Mar. Sci.* 1, 1-16.
- 552 McGlynn, S.E., 2017. Energy metabolism during anaerobic methane oxidation in ANME archaea.  
553 *Microbes Environ.* 32, 5-13.
- 554 McGlynn, S.E., Chadwick, G.L., Kempes, C.P., Orphan, V.J., 2015. Single cell activity reveals  
555 direct electron transfer in methanotrophic consortia. *Nature* 526, 531-535.
- 556 Meulepas, R.J.W., Jagersma, C.G., Gieteling, J., Buisman, C.J.N., Stams, A.J.M., Lens, P.N.L.,  
557 2009a. Enrichment of anaerobic methanotrophs in sulfate-reducing membrane bioreactors.  
558 *Biotechnol. Bioeng.* 104, 458-470.
- 559 Meulepas, R.J.W., Jagersma, C.G., Khadem, A.F., Buisman, C.J.N., Stams, A.J.M., Lens, P.N.L.,  
560 2009b. Effect of environmental conditions on sulfate reduction with methane as electron donor by  
561 an Eckemförde Bay enrichment. *Environ. Sci. Technol.* 43, 6553-6559.
- 562 Milucka, J., Ferdelman, T.G., Polerecky, L., Franzke, D., Wegener, G., Schmid, M., Lieberwirth,  
563 I., Wagner, M., Widdel, F., Kuypers, M.M.M., 2012. Zero-valent sulphur is a key intermediate in  
564 marine methane oxidation. *Nature* 491, 541-546.
- 565 Musat, N., Halm, H., Winterholler, B., Hoppe, P., Peduzzi, S., Hillion, F., Horreard, F., Amann,  
566 R., Jørgensen, B.B., Kuypers, M.M.M., 2008. A single-cell view on the ecophysiology of  
567 anaerobic phototrophic bacteria. *PNAS* 105, 17861-17866.
- 568 Pérez, M., Álvarez-Hornos, F., Engesser, K., Dobsław, D., Gabaldón, C., 2016. Removal of 2-  
569 butoxyethanol gaseous emissions by biotrickling filtration packed with polyurethane foam. *New*  
570 *Biotechnol.* 33, 263-272.
- 571 Pernthaler, A., Pernthaler, J., Amann, R., 2004. Sensitive multi-color fluorescence in situ  
572 hybridization for the identification of environmental microorganisms, in: Kowalchuk, G., de  
573 Bruijn, F., Head, I., Akkermans, A., van Elsas, J.D. (Eds.), *Molecular Microbial Ecology Manual*.  
574 Springer, Dordrecht, pp. 711-726.
- 575 Pruesse, E., Quast, C., Knittel, K., Fuchs, B.M., Ludwig, W., Peplies, J., Glöckner, F.O., 2007.  
576 SILVA: a comprehensive online resource for quality checked and aligned ribosomal RNA  
577 sequence data compatible with ARB. *Nucleic Acids Res.* 35, 7188-7196.

- 578 Raghoebarsing, A.A., Pol, A., van de Pas-Schoonen, K.T., Smolders, A.J.P., Ettwig, K.F., Rijpstra,  
579 W.I.C., Schouten, S., Damsté, J.S.S., Op den Camp, H.J.M., Jetten, M.S.M., Strous, M., 2006. A  
580 microbial consortium couples anaerobic methane oxidation to denitrification. *Nature* 440, 918-  
581 921.
- 582 Rikmann, E., Zekker, I., Tenno, T., Saluste, A., Tenno, T., 2018. Inoculum-free start-up of biofilm-  
583 and sludge-based deammonification systems in pilot scale. *Environ. Sci. Technol.* 15, 133-148.
- 584 Reeburgh, W.S., 2007. Oceanic methane biogeochemistry. *Chem. Rev.* 107, 486-513.
- 585 Ruff, S. E., Kuhfuss, H., Wegener, G., Lott, C., Ramette, A., Wiedling, J., Knittel, K., Weber, M.,  
586 2016. Methane seep in shallow-water permeable sediment harbors high diversity of anaerobic  
587 methanotrophic communities, Elba, Italy. *Front. Microbiol.* 7, 374.
- 588 Schauer, R., Røy, H., Augustin, N., Gennerich, H.-H., Peters, M., Wenzhoefer, F., Amann, R.,  
589 Meyerdierks, A., 2011. Bacterial sulfur cycling shapes microbial communities in surface  
590 sediments of an ultramafic hydrothermal vent field. *Environ. Microbiol.* 13, 2633-2648.
- 591 Scheller, S., Yu, H., Chadwick, G.L., McGlynn, S.E., Orphan, V.J., 2016. Artificial electron  
592 acceptors decouple archaeal methane oxidation from sulfate reduction. *Science* 351, 703-707.
- 593 Schloss, P.D., Westcott, S.L., 2011. Assessing and improving methods used in operational  
594 taxonomic unit-based approaches for 16S rRNA gene sequence analysis. *Appl. Environ.*  
595 *Microbiol.* 77, 3219-3226.
- 596 Schreiber, L., Holler, T., Knittel, K., Meyerdierks, A., Amann, R., 2010. Identification of the  
597 dominant sulfate-reducing bacterial partner of anaerobic methanotrophs of the ANME-2 clade.  
598 *Environ. Microbiol.* 12, 2327-2340.
- 599 Song, Z.-Q., Wang, F.-P., Zhi, X.-Y., Chen, J.-Q., Zhou, E.-M., Liang, F., Xiao, X., Tang, S.K.,  
600 Jiang, H.C., Zhang, C.L., Dong, H., Li, W.J., 2013. Bacterial and archaeal diversities in Yunnan  
601 and Tibetan hot springs, China. *Environ. Microbiol.* 15, 1160-1175.
- 602 Stahl, D.A., Amann, R.I., 1991. Development and application of nucleic acid probes, in:  
603 Stackebrandt, E., Goodfellow, M. (Eds.), *Nucleic Acid Techniques in Bacterial Systematics*. John  
604 Wiley & Sons Ltd, Chichester, UK, pp. 205-248.
- 605 Suarez-Zuluaga, D.A., Weijma, J., Timmers, P.H.A., Buisman, C.J.N., 2014. High rates of  
606 anaerobic oxidation of methane, ethane and propane coupled to thiosulphate reduction. *Environ.*  
607 *Sci. Pollut. Res.* 22, 3697-3704.
- 608 Tenno, T., Rikmann, E., Uiga, K., Zekker, I., Mashirin, A., Tenno, T., 2018. A novel proton  
609 transfer model of the closed equilibrium system  $H_2O-CO_2-CaCO_3-NH_x$ . *P. Est. Acad. Sci.* 67,  
610 26-270.
- 611 Timmers, P.H., Gieteling, J., Widjaja-Greefkes, H.A., Plugge, C.M., Stams, A.J., Lens, P.N.L.,  
612 Meulepas, R.J., 2015a. Growth of anaerobic methane-oxidizing archaea and sulfate-reducing

- 613 bacteria in a high-pressure membrane capsule bioreactor. *Appl. Environ. Microbiol.* 81, 1286-  
614 1296.
- 615 Timmers, P.H., Suarez-Zuluaga, D.A., van Rossem, M., Diender, M., Stams, A.J., Plugge, C.M.,  
616 2015b. Anaerobic oxidation of methane associated with sulfate reduction in a natural freshwater  
617 gas source. *ISME J.* 10, 1400-1412.
- 618 Timmers, P.H., Welte, C.U., Koehorst, J.J., Plugge, C.M., Jetten, M.S.M., Stams, A.J.M., 2017.  
619 Reverse methanogenesis and respiration in methanotrophic archaea. *Archaea* 2017,1654237.
- 620 Wegener, G., Krukenberg, V., Riedel, D., Tegetmeyer, H.E., Boetius, A., 2015. Intercellular  
621 wiring enables electron transfer between methanotrophic archaea and bacteria. *Nature* 526,587-  
622 603.
- 623 Wegener, G., Krukenberg, V., Ruff, S.E., Kellermann, M.Y., Knittel, K., 2016. Metabolic  
624 capabilities of microorganisms involved in and associated with the anaerobic oxidation of  
625 methane. *Front. Microbiol.* 7, 46.
- 626 Wehrmann, L.M., Risgaard-Petersen, N., Schrum, H.N., Walsh, E.A., Huh, Y., Ikehara, M., Pierre,  
627 C., D'Hondt, S., Ferdelman, T.G., Ravelo, A.C., Takahashi, K., Zarikian, C., 2011. Coupled  
628 organic and inorganic carbon cycling in the deep seafloor sediment of the north-eastern bering  
629 sea slope. *Chem. Geol.* 284, 251-261.
- 630 Widdel, F., Bak, F., 1992. Gram negative mesophilic sulfate reducing bacteria, in: Balows, A.,  
631 Truper, H., Dworkin, M., Harder, K., Schleifer, H. (Eds.), *The prokaryotes: a handbook on the*  
632 *biology of bacteria: ecophysiology, isolation, identification, applications.* Springer-Verlag, New  
633 York, USA, pp. 3352-3378.
- 634 Zekker, I., Kivirüüt, Rikmann, E., Mandel, A., Jaagura, M., Tenno, T., Artemchuk, O., Rubin, S.,  
635 Tenno, T., 2018. Enhanced efficiency of nitrifying-anammox sequencing batch reactor achieved  
636 at low decrease rates of oxidation–reduction potential. *Environ. Eng. Sci.*  
637 <https://doi.org/10.1089/ees.2018.0225>.
- 638 Zhang, Y., Maignien, L., Zhao, X., Wang, F., Boon, N., 2011. Enrichment of a microbial  
639 community performing anaerobic oxidation of methane in a continuous high-pressure bioreactor.  
640 *BMC Microbiol.* 11, 1-8.
- 641 Zhu, J., Wang, Q., Yuan, M., Tan, G.-Y.A., Sun, F., Wang, C., Wu, W., Lee, P.-H., 2016.  
642 Microbiology and potential applications of aerobic methane oxidation coupled to denitrification  
643 (AME-D) process: a review. *Water Res.* 90, 203-215.

644 **Tables**

645 **Table 1.** Sulfide production, SR and AOM rates, and the sulfur and carbon balance for each  
 646 different phase in the BTF and for the activity tests with  $^{13}\text{CH}_4$ , controls without  $\text{CH}_4$  but with  $\text{N}_2$   
 647 in the headspace and controls without biomass.

648

Incubation description and duration		Sulfide production rate (mmol l <sup>-1</sup> day <sup>-1</sup> )	SR rate (mmol l <sup>-1</sup> day <sup>-1</sup> )	Sulfur balance	AOM rate (mmol l <sup>-1</sup> day <sup>-1</sup> )	Carbon balance
<b>BTF (238 days)</b>						
Phase I 0–61 days		0.00 ± 0.00	0.05 ± 0.00	0.33	0.19 ± 0.09	0.76
Phase II 61–119 days		0.08 ± 0.00	0.12 ± 0.00	0.61	0.28 ± 0.02	0.88
Phase III 119–160 days		0.17 ± 0.01	0.29 ± 0.03	0.96	0.34 ± 0.06	0.99
Phase IV 160–214 days		0.17 ± 0.01	0.26 ± 0.03	0.98	0.37 ± 0.03	0.97
Phase V 214–238 days		0.15 ± 0.01	0.26 ± 0.04	0.98	0.31 ± 0.02	0.87
<b>Activity assays (42 days)</b>						
Incubation with $^{13}\text{CH}_4$	0-42 days	0.09 ± 0.01	0.10 ± 0.03	0.99	0.16 ± 0.01	0.99
Incubation without $^{13}\text{CH}_4$	0-20 days	0.08 ± 0.02	0.05 ± 0.03	0.99	Not detected	0.99
	20-42 days	Not detected	Not detected	0.99		
Incubation without biomass	0-42 days	Not detected	Not detected	0.99	Not detected	0.99

649

650

651 **Table 2.** Overview of inocula and bioreactor types used in AOM studies.

652

Inoculum	Bioreactor type	Operation time (d)	AOM rate ( $\mu\text{mol l}^{-1} \text{ day}^{-1}$ )	Reference
Alpha Mound, Gulf of Cadiz	Polyurethane foam and pall rings packed BTF	238	160	This study
Alpha Mound, Gulf of Cadiz	Polyurethane foam packed BTF	248	8.4	Cassarini et al., 2018
Gingsburg mud volcano, Gulf of Cadiz	Polyurethane foam packed BTF	200	10	Bhattacharai et al., 2018b
Nankai Trough	Down-flow hanging sponge (DHS) bioreactor	2013	$0.375 \mu\text{mol g}_{\text{dw}}^{-1} \text{d}^{-1}$	Aoki et al., 2014
Ginsburg mud volcano, Gulf of Cadiz	External ultrafiltration membrane bioreactor	726	$1.2 \mu\text{mol g}_{\text{dw}}^{-1} \text{d}^{-1}$	Bhattacharai et al., 2018a

653

654 **Figure legends**

655 **Figure 1.** Schematic of a biotrickling filter (BTF) configuration for anaerobic methane oxidation  
656 coupled to thiosulfate reduction. The filter bed (5.6 l) is packed with polyurethane foam cubes and  
657 polypropylene pall. SP: sampling port.

658 **Figure 2.** Profiles of different process parameters monitored during the operation of the BTF with  
659 methane as electron donor and sulfate as electron acceptor: (A) pH, (B) sulfate and sulfide, and  
660 (C) carbon dioxide concentration measured as [carbon dioxide outlet – carbon dioxide inlet]. The  
661 vertical lines represent the different phases in bioreactor operation; I: days 0–61, II: days 61–119,  
662 III: days 119–160, IV: days 160–214, V: days 214–238. The start of each phase indicates the days  
663 at which the mineral medium was replaced.

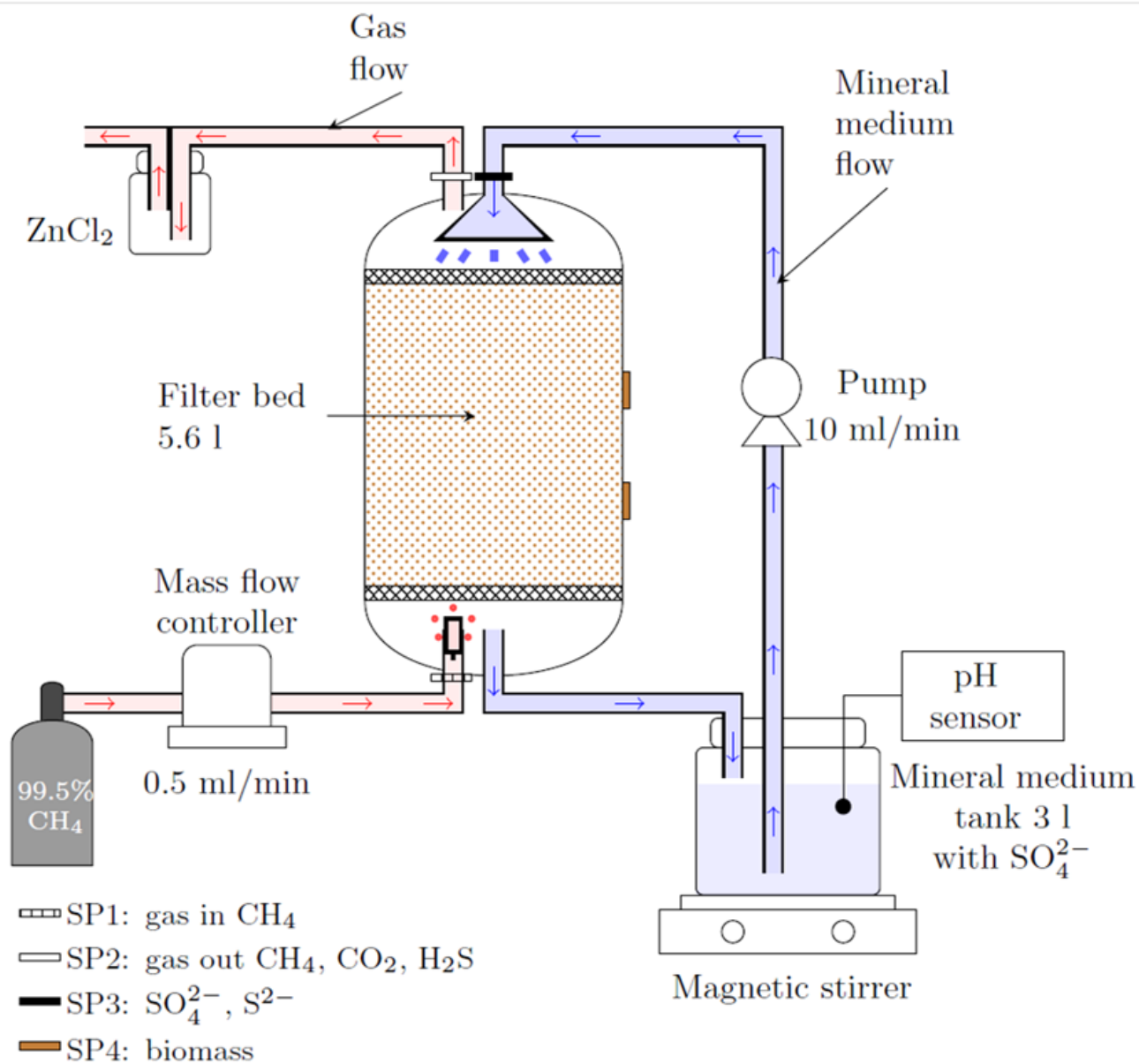
664 **Figure 3.**

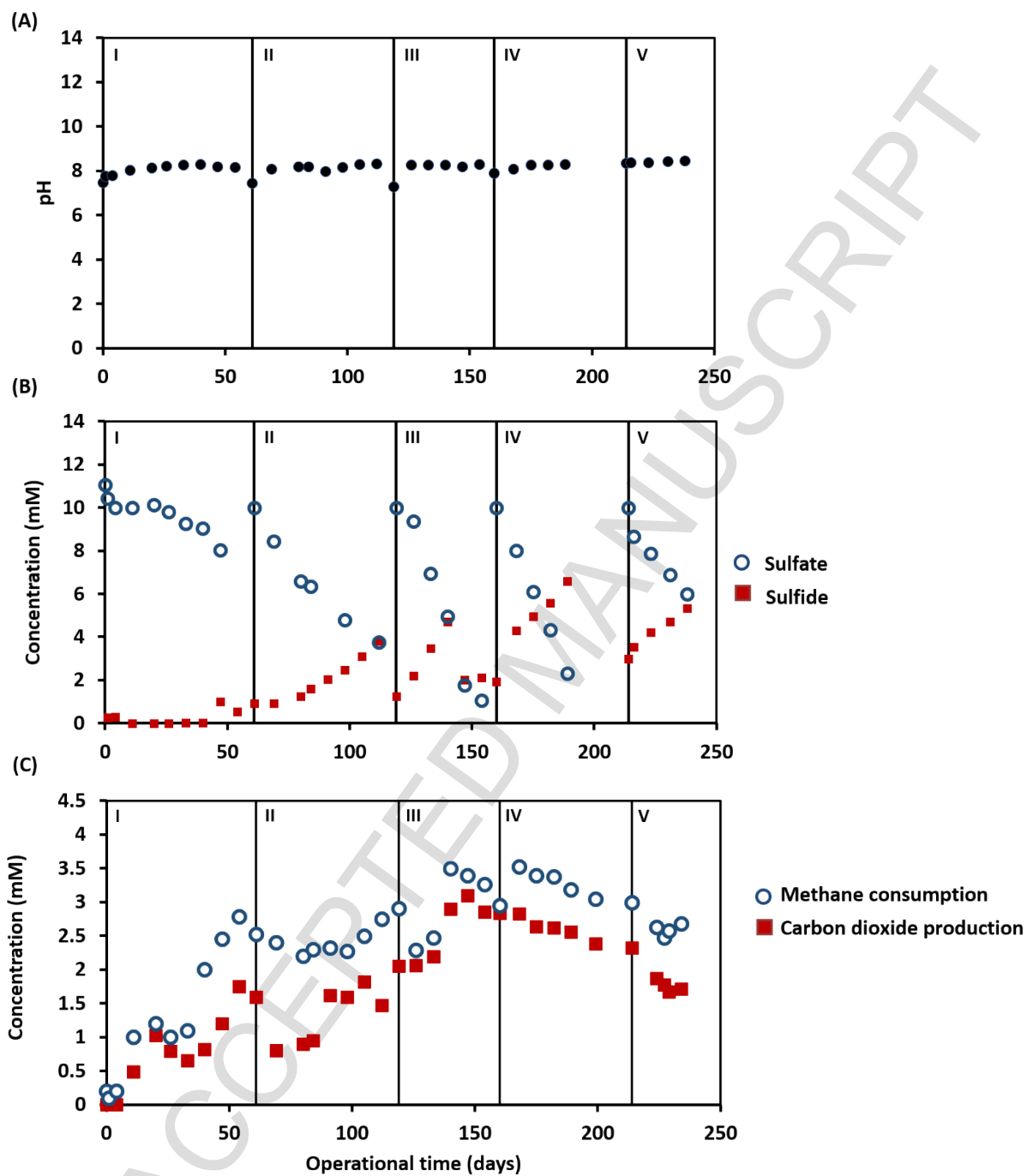
665 Topmost abundant 16S rRNA sequences showing the phylogenetic affiliation up to gene level as  
666 derived by high-throughput sequencing of archaea (a) and bacteria (b) at the start (t=0) and at the  
667 end (t = 238 d) of the BTF operation.

668 **Figure 4.** Batch activity assay profiles for the BTF with sulfate as electron acceptor and methane  
669 as the sole electron donor during the activity test for the batches incubated with  $^{13}\text{CH}_4$  (triplicates)  
670 and controls. *Dotted lines* show the controls without  $\text{CH}_4$ , but with  $\text{N}_2$  in the headspace and *dashed*  
671 *lines* showed controls without biomass. (A) Sulfide and sulfate profiles and (B) the total dissolved  
672 inorganic carbon (DIC) production calculated from the produced  $^{13}\text{CO}_2$ . Error bars represent the  
673 standard deviation of triplicate measurements.

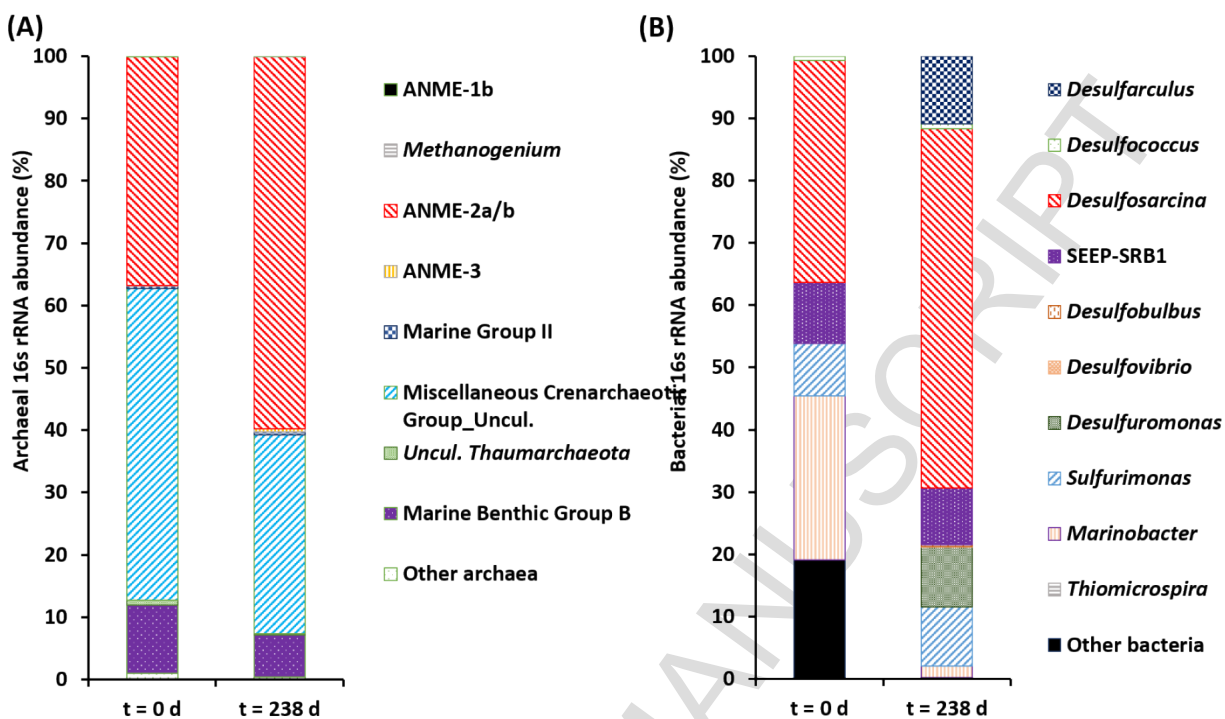
674 **Figure 5.** Catalyzed reporter deposition - fluorescence *in situ* hybridization (CARD-FISH)  
675 analysis during the activity assays. CARD-FISH images (A–D) from ANME-2 in red color and

676 *Desulfosarcina/Desulfococcus* group (DSS) in green after 42 days of incubation with  $^{13}\text{CH}_4$ .  
677 White scale bar representing 10 $\mu\text{m}$ . (E) The number of single cells stained by specific CARD-  
678 FISH probe over DAPI (4', 6-diamidino-2-phenylindole, all cells) stained cells during the activity  
679 assays incubated with  $^{13}\text{CH}_4$  (triplicates). Error bars indicate the standard deviation (n=3). CARD-  
680 FISH probes used: ARC 915 (for all archaea), EUB 338-I-II-III (for all bacteria), ANME-2 538  
681 (for ANME clade: ANME-2) and DSS658 (for a specific group of SRB: *Desulfosarcina* /  
682 *Desulfococcus*, DSS).

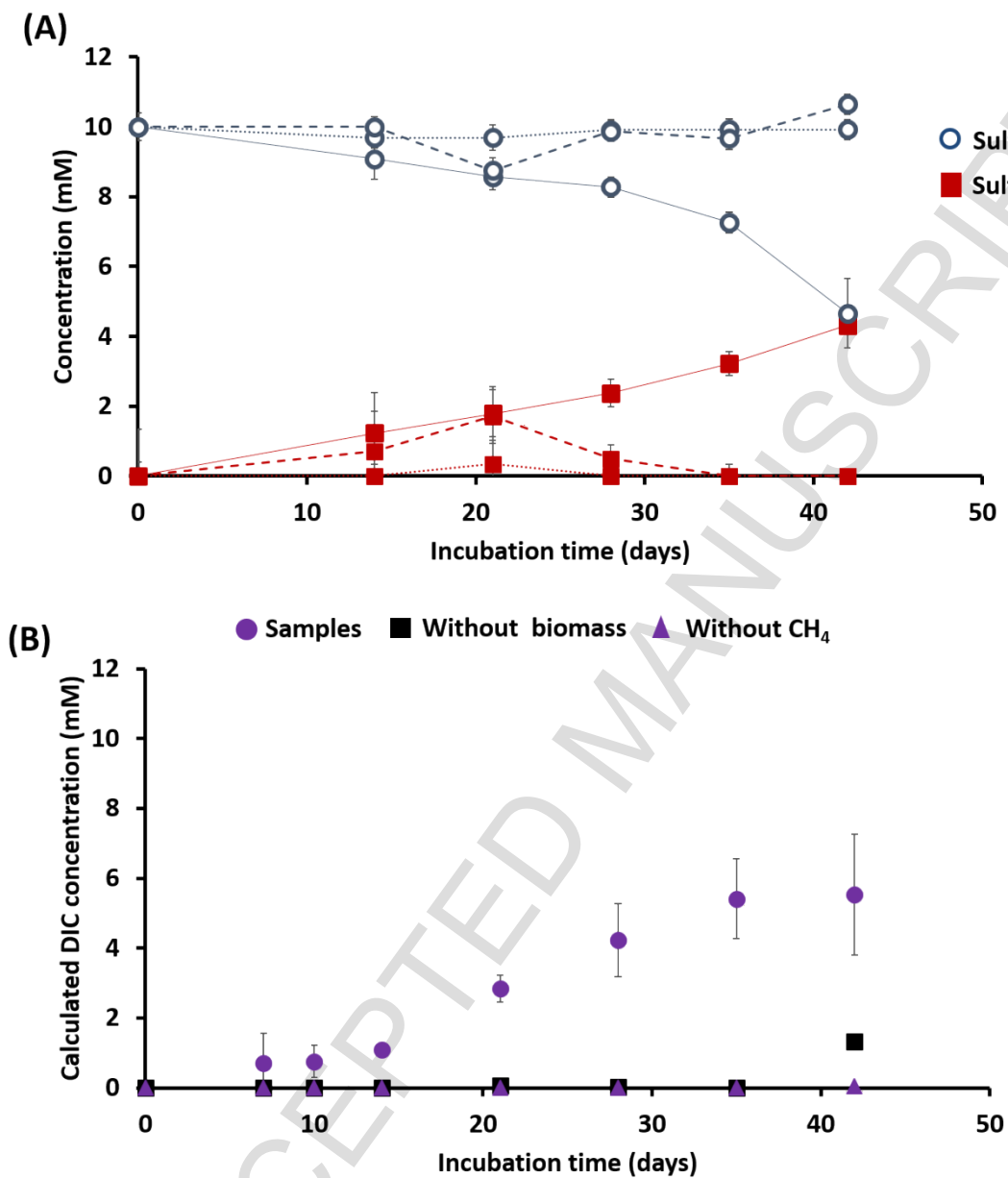
683 **Figure 1**684  
685

686 **Figure 2**

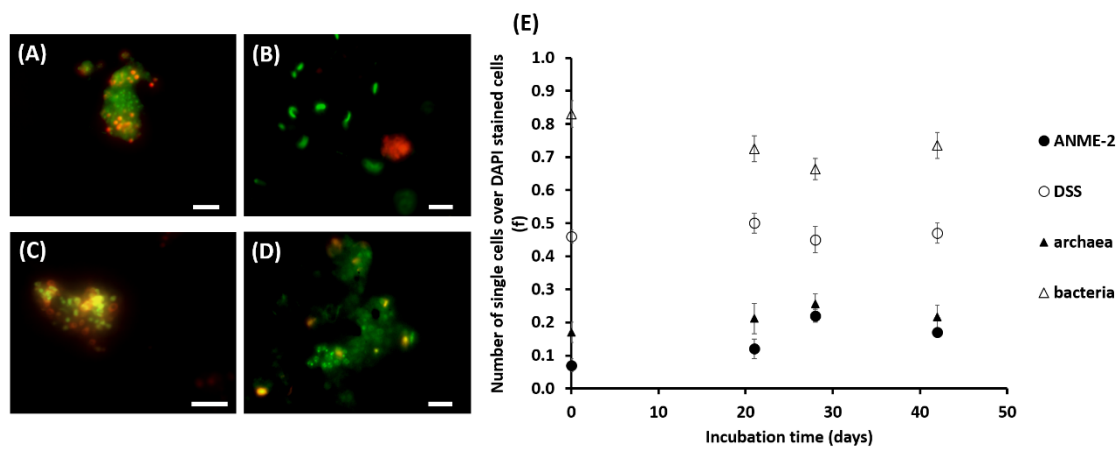
687

688 **Figure 3**

689

690 **Figure 4**

691

692 **Figure 5**

693

694

ACCEPTED MANUSCRIPT

